Laser-assisted printing of alginate long tubes and annular constructs

2013 Biofabrication 5 015002

(http://iopscience.iop.org/1758-5090/5/1/015002)

Biofabrication **5** (2013) 015002 (8pp) doi:10.1088/1758-5082/5/1/015002

Laser-assisted printing of alginate long tubes and annular constructs

Jingyuan Yan[1], **Yong Huang**[1,3] **and Douglas B Chrisey**[2]

[1] Department of Mechanical Engineering, Clemson University, Clemson, SC 29634, USA
[2] Department of Materials Science and Engineering, Rensselaer Polytechnic Institute, Troy, NY 12180, USA

E-mail: yongh@clemson.edu

Received 15 May 2012
Accepted for publication 29 October 2012
Published 21 November 2012
Online at stacks.iop.org/BF/5/015002

Abstract
Laser-assisted printing such as laser-induced forward transfer has been well studied to pattern or fabricate two-dimensional constructs. In particular, laser printing has found increasing biomedical applications as an orifice-free cell and organ printing approach, especially for highly viscous biomaterials and biological materials. Unfortunately, there have been very few studies on the efficacy of three-dimensional printing performance of laser printing. This study has investigated the feasibility of laser tube printing and the effects of sodium alginate concentration and operating conditions such as the laser fluence and laser spot size on the printing quality during laser-assisted printing of alginate annular constructs (short tubes) with a nominal diameter of 3 mm. It is found that highly viscous materials such as alginate can be printed into well-defined long tubes and annular constructs. The tube wall thickness and tube outer diameter decrease with the sodium alginate concentration, while they first increase, then decrease and finally increase again with the laser fluence. The sodium alginate concentration dominates if the laser fluence is low, and the laser fluence dominates if the sodium alginate concentration is low.

(Some figures may appear in colour only in the online journal)

1. Introduction

Organ transplantation has been well developed over the last several decades, and it has saved the life of numerous patients with diseased organs. However, organ transplantation itself is limited by various hurdles, such as pathogen transfer, immune rejection, high cost and especially the donor shortage. Fortunately, organ printing, an additive manufacturing technique-based approach, has emerged as a promising technological solution to tackle some of these hurdles. As envisioned, three-dimensional (3D) scaffold-free tissue or organ constructs will be fabricated [1–4] in a layer-by-layer fashion using patient's cells based on the computer-aided model of patient-specific organs.

Different 3D scaffold-free heterogeneous structures can be fabricated using various 3D additive printing technologies, for example, jet-based laser printing [3] and inkjet printing [5]. During 3D additive printing, constituent materials of the structure or their precursors are dispensed three dimensionally to construct the 3D product layer-by-layer based on computer-aided models. Currently, 3D additive printing and its variations have been implemented to create various 3D patterns and structures and found numerous engineering and biomedical applications [3, 6, 7]. One of its most exciting applications is to fabricate human tissues and organs suitable for regeneration, repair and replacement of damaged, injured or lost cells [1], which is generally called cell/organ printing or bioprinting.

Generally, 3D additive printing-based organ printing or 3D organ printing can be implemented using orifice-based and orifice-free approaches. As the widely used orifice-based fabrication approach, inkjetting has been applied to fabricate various biological patterns or constructs such as alginate tubes [8, 9]. However, orifice-based printing may experience a great difficulty in printing viscous biological materials such as alginate, which may clog the nozzle during printing. For example, only sodium alginate with concentrations lower than

[3] Author to whom any correspondence should be addressed.

2% is recommended for inkjetting [10–12]. As such, orifice-free techniques should be developed for the printing of viscous biomaterials and biological materials, which are common constituents of many biological constructs. Fortunately, laser-assisted printing/direct writing, an orifice-free printing approach developed based on laser-induced forward transfer (LIFT), has been investigated to print and pattern different materials including biomaterials and biological materials [3, 13–20]. LIFT serves as a complementary clogging-free bioprinting technique to inkjetting for some viscous printing applications [17].

During LIFT, a laser pulse is focused perpendicularly through the backside of a quartz support-based ribbon, which consists of an optically transparent quartz disc and a coated material (ribbon coating and/or a layer of energy absorbing material) to be transferred. The ribbon coating is then locally heated by the laser beam, immediately generating a small vapor pocket/bubble at the interface of the quartz disc and coating. The generated bubble then expands rapidly and ejects part of the coating material downwards, forming a jet/droplet for deposition [21, 22]. While it has been proved to be a viable technique in printing various cells [14, 15, 18–20], LIFT has been pioneered to print different biological patterns. For example, Koch *et al* [15] made a chess board pattern using fibroblasts (NIH 3T3) and keratinocytes (HaCaT); Gruene *et al* [23] fabricated two-dimensional (2D) word and grid patterns using porcine bone marrow-derived mesenchymal stem cells; Catros *et al* [24] laser printed human osteoprogenitors (HOPs) into 2D and 3D annular patterns; and Koch *et al* [25] printed a 3D layered construct (homogeneous along the horizontal plane) based on the alternating layers of HaCaT keratinocytes dyed with different colors. However, laser-assisted printing has not been studied to fabricate 3D scaffold-free tubular constructs thus far. In the field of biofabrication, the fabrication of hollow cellular tubes to mimic vascular structures has been widely recognized as not only the first logical step toward successful organ printing, but also a critical indicator of the feasibility of the envisioned organ printing technology [26].

The objective of this study is to study the feasibility of laser printing of alginate tubes and investigate the effects of sodium alginate (NaAlg) concentration and operating conditions such as the laser fluence and laser spot size on the printing quality. In this study, sodium alginate and calcium chloride were used as the gel precursor and gel reactant solution, respectively, for the making of alginate tubes due to their wide applications in the healthcare field. The paper is organized as follows. First, 3D printing technologies are reviewed in the context of biomedical applications. Second, the experimental setup and design for 3D laser printing is explained. After the feasibility of tube printing is introduced, the effects of sodium alginate concentration and operating conditions on the printing quality, particularly the tube outer diameter and tube wall thickness, are discussed respectively. Finally, the conclusions and future work are presented. This study, serving as a preliminary investigation toward 3D organ printing, has attempted to print scaffold-free straight alginate tubes using LIFT.

2. Materials and methods

2.1. Materials

Alginate, particularly, sodium alginate, has been used as a constituent of bioink in bioprinting [8, 27, 28]. As such, sodium alginate (product number W201502, Sigma-Aldrich, St. Louis, MO), which has a molecular weight range of 20–40 kDa, and deionized water were used to prepare the sodium alginate solution with different concentrations: 1%, 2%, 4%, 6% and 8% (w/v). High concentration alginate solutions were used in order to simulate application scenarios during the printing of viscous hydrogel materials. Calcium chloride dihydrate (Sigma-Aldrich, St. Louis, MO), a cross-linking agent, was used as a source of calcium ions to initiate gelation once the sodium alginate is merged into a calcium chloride bath. It should be noted that while alginate is not an ideal material for living tissue construction, it is a good hydrogel material for proof-of-concept studies. If not specified, the calcium chloride concentration was 2% (w/v) in this study.

2.2. Experiment apparatus and fabrication mechanism

Matrix-assisted pulsed-laser evaporation direct-write (MAPLE DW), a typical LIFT practice [16, 21], has been of particular interest in this study as the laser-assisted printing technique. As shown in figure 1, part of the alginate solution, which was coated on the bottom side of the quartz disc-based ribbon, was ejected due to the laser pulse-induced high-pressure bubble [21] and deposited on the receiving platform inside the calcium chloride container. The laser printing setup contained a 193 nm, 12 ns (full-width half-maximum) ArF excimer laser (Coherent ExciStar, Santa Clara, CA) and an optical beam delivery system. The laser spot size was controlled at 150 μm in diameter, and the actual laser fluence was measured using a Coherent FieldMax power/energy meter (Coherent, Portland, OR). The laser repetition rate was set at 10 Hz. Quartz disc (Edmund optics, Barrington, NJ) with 85% transmittance for 193 nm wavelength laser beams was used to make the ribbon, which had the alginate coating on the bottom side. The sodium alginate solution was coated using a film applicator (MTI, Richmond, CA), resulting in the ribbon coating with a thickness of 100 μm.

During the printing process, the landing location for alginate droplets being deposited was the newly printed top layer of the construct being printed. The direct writing height, the distance between the ribbon and the liquid level, was set at 1 mm to optimize the printing quality in terms of the feature size of the deposited feature (tube wall). The top layer was controlled around 0.5 mm above the liquid level to avoid possible contact between the ribbon coating and the calcium chloride solution, resulting in a 1.5 mm gap between them. Once deposited, the platform moved downwards to submerge into the calcium chloride solution to fully gelatinize the newly deposited alginate droplet-based layer. Subsequently, this newly deposited layer was raised 0.5 mm above the liquid level before continuing the subsequent round of printing; thus, the platform moved down around 25 μm between any two consecutive printing positions, meaning a layer thickness of

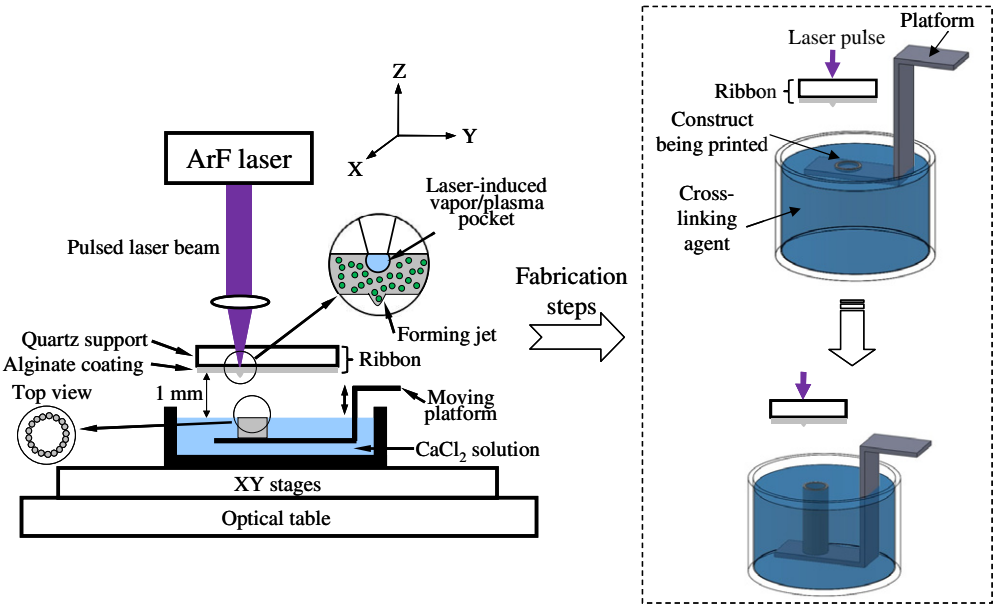

Figure 1. Schematics of laser-assisted printing experimental setup and fabrication steps.

25 μm. This process repeated until a construct was made. In addition, the jet formation process was also monitored using JetXpert (ImageXpert Inc., Nashua, NH).

The relative motion between the ribbon and the receiving container was controlled using *XY* translational stages (Aerotech, Pittsburgh, PA). The laser beam horizontal traveling speed was set at 100 mm min^{-1}, resulting in a 167 μm spatial distance between two consecutive pulses. The downward motion of the platform, on which the construct was printed, was precisely controlled using a *Z* axis stage (Thorlabs, Newton, NJ). The post-printing measurements were conducted immediately after the making of alginate tubes, and the residual liquid inside tubes was removed out using a pipette. For each tube, four measurements were conducted equidistantly along the circumferential direction to obtain the averaged wall thickness and tube outer diameter. Under each fabrication condition, three tubes were made, and the reported wall thickness and tube diameter were the averaged values of those of three tubes.

2.3. Design of experiments

In this study, some long, straight alginate tubes (6 mm in height, 240 layers) were fabricated first to prove the feasibility in making such tubes. Then a parametric study was conducted to appreciate the effects of material properties and operating conditions on the printing quality by printing annular constructs or short tubes (around 1 mm in height, 20 layers). It should be pointed out that the construct height is not proportional to the number of layers due to the increasing wall thickness as the height increases. The printing quality herein is evaluated based on the wall thickness and diameter of printed tubes, and the annular constructs (short tubes) are discussed as tubes for convenience in the following sections. For all experiments, the concentration of calcium chloride solution was 2%. For all tubes, the nominal tube diameter, which is the diameter defined by the center of laser beam spot, was controlled at 3 mm.

The parametric study was implemented in three different setups to appreciate the effects of sodium alginate concentration, laser fluence and laser spot size on the printing quality. The first setup was to study the effect of sodium alginate concentration on the printing quality, and annular constructs were printed using 2%, 4%, 6% and 8% sodium alginate solutions while keeping the laser fluence at 1437 $\pm$ 28 mJ cm^{-2}. The second setup was to study the effect of laser fluence, and the laser fluence was varied as follows: 1149 $\pm$ 31, 1437 $\pm$ 28[2], 1698 $\pm$ 45, 2009 $\pm$ 45 and 2286 $\pm$ 45 mJ cm^{-2} for each of 2%, 4%, 6% and 8% sodium alginate solutions. The third setup was to study the effect of laser spot size, and a 50 μm (in diameter) spot size was studied in addition to the nominal spot size (150 μm) for 2%, 4%, 6% and 8% sodium alginate solutions, respectively, under a laser fluence of 2286 $\pm$ 45 mJ cm^{-2}.

3. Experimental results and discussion

3.1. Representative alginate tubes

Figure 2(*a*) shows a representative alginate long tube printed using the proposed laser printing technique, and the height of the tube is about 6 mm. This tube was printed using an 8% sodium alginate solution under a laser fluence of 1698 $\pm$ 45 mJ cm^{-2}. The tube was made with 240 layers and it has an average wall thickness of 0.8 mm and an outer diameter of 3.3 mm. For further illustration, figures 2(*b*) and (*c*) show the top and side views of two different tubes. Generally, the wall surface is rough and the tube top layer is not flat, which might be due to the pulse instability of the excimer laser and/or the spreading of deposited droplets during landing. While some promising results have been achieved in terms of the overall feasibility, some process optimization work is expected in future studies in order to improve the overall printing stability and quality.

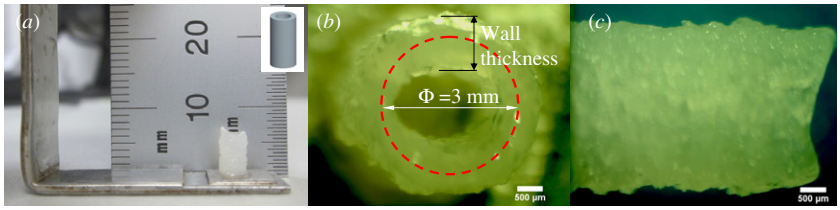

Figure 2. (*a*) A representative tube fabricated using the proposed laser printing technique, (*b*) top view of the tube and (*c*) side view of the tube.

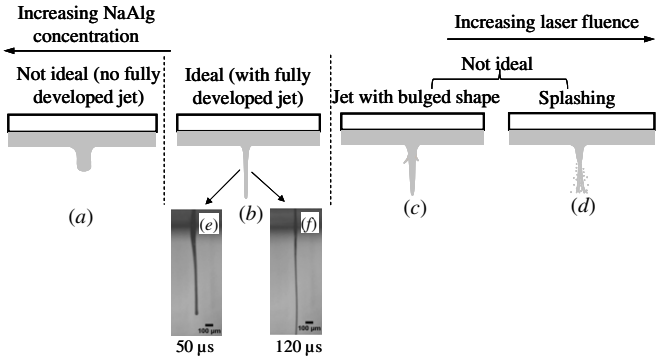

Figure 3. Jet formation regimes and representative jet formation observations.

The entire process of laser-assisted printing can be divided into three steps: bubble formation, jet formation/breakup and jet/droplet landing. It should be noted that during laser-assisted direct writing such as LIFT, the material transfer and deposition can be due to either formed droplets [13, 29] or the contact between formed long, thin jet and the receiving substrate [30, 31] depending on the direct writing height and material properties. In this study, the constructs were fabricated mostly due to the contact of alginate jets based on the imaging study of the printing process. Upon landing, both mechanical impact/spreading and chemical gelation happen simultaneously.

The jet formation process during laser printing of alginate solution can be classified into four different scenarios, as shown in figure 3, depending on the laser fluence and the sodium alginate concentration. During the printing process, once the energy of incident laser pulse is absorbed by the sodium alginate solution-based ribbon coating, a high-pressure, high-temperature bubble might form and further expand within the coating due to sublimation pressure [21, 22, 32]. Fully developed jets only form under certain operating conditions for a given sodium alginate solution. If the laser fluence is too low and/or the sodium alginate concentration is too high, which means a more viscous fluid, it is difficult for a bubble to fully form and/or expand before it diminishes [33]. As a result, a jet may not fully form and further develop (figure 3(*a*)) since there is no enough kinetic energy provided by the expanding bubble. Instead, a jet, if formed, retracts back after the bubble diminishes. If the laser fluence is too high and/or the sodium alginate concentration is too low, it is also difficult to form a well-developed jet as desired. Rapid, powerful bubble expansion may lead to a bulged shape [34] and even splashing [21, 35] as shown in figures 3(*c*) and (*d*), which is not ideal for pattern and construct printing. Only with some combinations of laser fluence and sodium alginate concentration, a jet can be fully developed as shown in figure 3(*b*). The laser fluence determines the jet kinetic energy, and the sodium alginate concentration affects the viscous dissipation energy and the surface tension force. When the jet kinetic energy is higher than that of viscous dissipation, a jet forms; when the surface tension effect dominates and leads to the Rayleigh instability, the jet breaks up, forming flying droplets. It should be noted that if the jet kinetic energy is too high, it may end up with a bulged jet or splashing, which is not good for good printing performance.

To further illustrate the jet formation process, two representative jet observations are shown in figures 3(*e*) and (*f*) during the printing of 8% sodium alginate solution under a laser fluence of 1183 ± 67 mJ cm^{-2}, taken at 50 and 120 μs, respectively. In this study, the jet fed alginate solution on the deposition location and broke up after deposition as reported in a previous study [36] instead of flying droplets. Both fluid properties and operating conditions affect the size of forming jets and the resolution of the printed gel structure.

3.2. Effect of sodium alginate concentration

To appreciate the effect of sodium alginate concentration on the tube printing quality, annular constructs (or short tubes) with a height of around 1 mm were printed from sodium alginate solutions with different concentrations: 2%, 4%, 6% and 8%. Some of printed constructs are shown in figures 4(*a*) and (*b*) (150 μm laser spot size) and figures 4(*c*) and (*d*) (50 μm laser spot size) under a laser fluence of 1437 ± 28 mJ cm^{-2}. It can be seen that the printing quality increased with the increase of sodium alginate concentration. As observed but not shown herein, the 1% sodium alginate solution did not yield any good structure under all operating conditions investigated; only a bulky gel stack was obtained instead of a hollow cylindrical tube. Although annular constructs were formed using the 2% sodium alginate solution, the construct quality was poor with a rough tube surface and non-uniform wall thickness as seen in figures 4(*a*) and (*c*). With the increase of sodium alginate concentration, the tube surface became smoother, and the construct shape became better defined. Apparently, higher concentration sodium alginate solutions (6% and 8%) yielded a better printing quality as seen in figures 4(*b*) and (*d*). The tube wall thickness and outer diameter are shown in figure 5 as the sodium alginate concentration increases. In the following thickness and/or diameter plots (figures 5–7), the error bars represent the

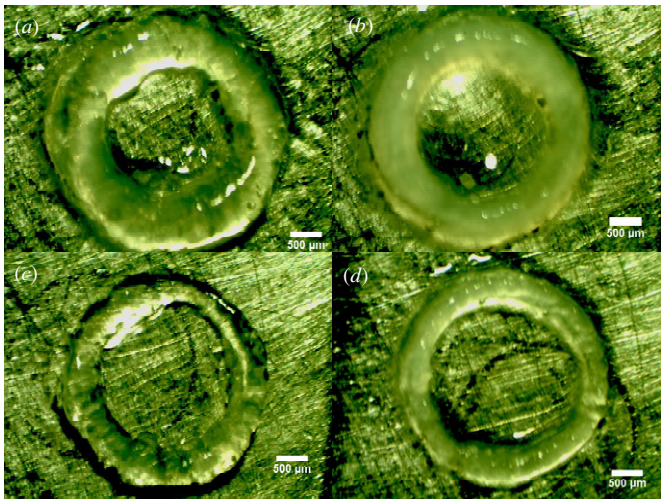

Figure 4. Printed annular constructs/short tubes made from sodium alginate solutions with different concentrations under a laser fluence of 1437 ± 28 mJ cm^{-2}: (*a*) 2%, (*b*) 8%, (*c*) 2% (50 μm laser spot size) and (*d*) 8% (50 μm laser spot size).

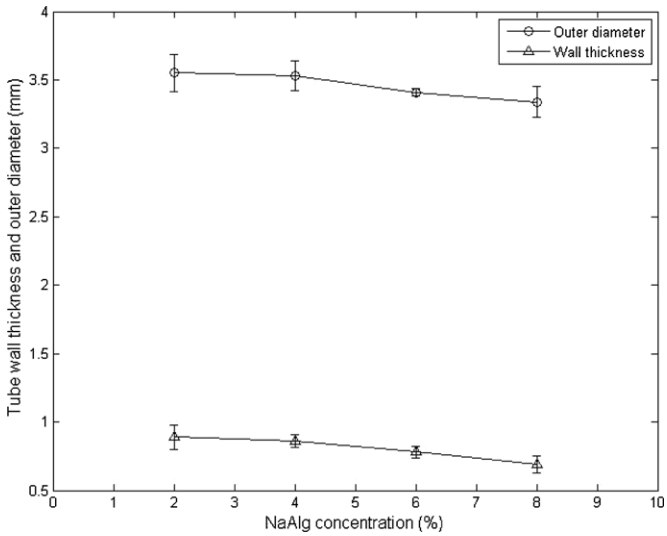

Figure 5. Tube wall thickness and outer diameter as a function of sodium alginate concentration (laser fluence 1437 ± 28 mJ cm^{-2}).

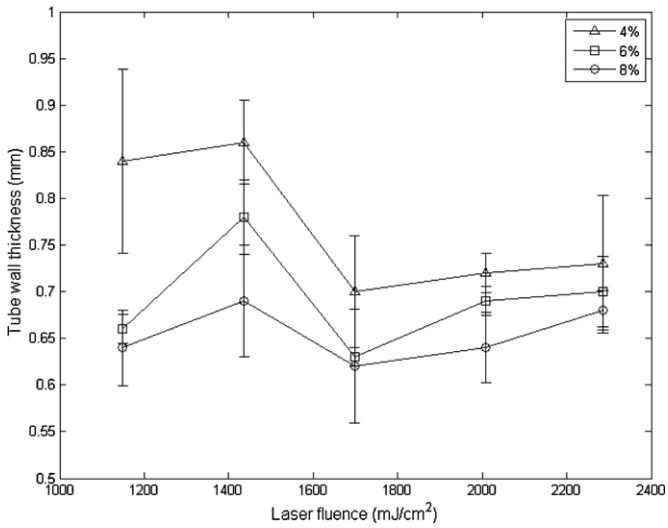

Figure 6. Tube wall thickness as a function of laser fluence.

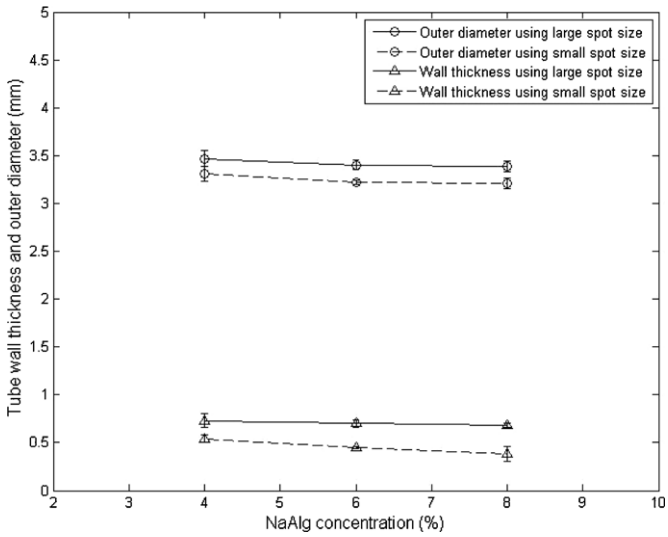

Figure 7. Tube outer diameter and wall thickness under different spot sizes with a laser fluence of 2286 ± 45 mJ cm^{-2}.

standard deviation (± one sigma) of the tube wall thickness and outer diameter. Herein the tube wall thicknesses were 0.89, 0.86, 0.78 and 0.68 mm, respectively, showing a decreasing trend and the tube outer diameters were 3.55, 3.52, 3.41 and 3.35 mm, respectively, also showing a decreasing trend. The discrepancy between the laser spot size (150 μm in diameter) and the resulted tube wall thickness (much larger than 150 μm) is attributed to the fluidic spreading of alginate jets when they landed on the previously deposited but gelatinized layer before their complete gelation.

A bubble may form upon the incidence of the laser pulse and eject the sodium alginate solution beneath as a jet if the forming bubble provides enough kinetic energy. As the sodium alginate concentration of the ribbon coating increases, the fluid viscosity increases significantly too. For example, the viscosity may increase almost twenty-seven times comparing those of 2% and 6% sodium alginate solutions (94 ± 1 versus 2618 ± 14 mPa s) [17]. A higher viscosity of the ribbon coating indicates a more pronounced viscous damping effect, resulting in a smaller ejection force for the transfer of alginate solution since more laser energy absorbed is consumed to overcome the viscous dissipation. As such, it leads to fewer materials being ejected and a slower jet if formed. Fewer materials ejected means a smaller-diameter jet/droplet per pulse with high concentration sodium alginate solutions as observed in inkjetting sodium alginate solution [11]; in other words, a better printing resolution. Since the resolution of the printed pattern is also affected by the landing velocity of jet/droplet, a lower velocity is expected to minimize the spreading effect, which can be accomplished using a high concentration solution. In addition, a viscous sodium alginate jet/droplet is difficult to be spread upon landing, helping improve the printing resolution. On the other hand, a less viscous sodium alginate solution is also likely to have a bulged shape or induce splashing as shown in figures 3(*c*) and (*d*), deteriorating the printing quality. The effect of sodium alginate

concentration on the printing quality showed a similar trend under other laser fluences (1149 ± 34, 1698 ± 45, 2009 ± 45 and 2286 ± 45 mJ cm^{-2}). As discussed, a higher concentration alginate solution generally leads to a better printing resolution due to its higher viscosity and the resulting lower jet/droplet velocity if a jet can be successfully formed.

3.3. Effect of laser fluence

To appreciate the effect of laser fluence on the tube printing quality, annular constructs were further printed under the laser fluence level from 1149 ± 34 to 2286 ± 45 mJ cm^{-2}. There were no monotonic trends for both the wall thickness (figure 6) and diameter as the laser fluence varied, while the 1698 ± 45 mJ cm^{-2} laser fluence resulted in the smaller wall thickness and tube diameter. The wall thickness and diameter increased first, then decreased, and finally increased as the laser fluence increased. For the 2% sodium alginate solution, it was difficult to print a tubular structure under higher laser fluences (higher than 2009 ± 45 mJ/cm^2), so the related results were not reported in figure 6.

When the laser fluence increases, it may lead to the following phenomena: (1) more materials transferred per pulse, (2) a higher speed jet/droplet or a higher landing velocity, (3) a well-developed jet with a smaller diameter within a certain fluence range as shown in figures 3(*e*) and (*f*), and (4) bulged or splashing jet when the laser fluence is too high. While the third result may lead to a better resolution, the others may deteriorate the resolution. These results are kinds of competing factors in determining the pattern resolution herein. When the laser fluence is relatively low, the first and second phenomena dominate, resulting in an increasing wall thickness as observed. When the laser fluence is relatively high, the fourth result dominates, also resulting in an increasing wall thickness as observed. Such an increasing trend as the external stimulation (such as the driving voltage in inkjetting) increases is also very common in inkjetting [11, 37]. When the laser fluence is right to induce a well-developed jet, the stretching effect under a high inertia force may dominate and lead to a smaller wall thickness. As discussed, the printing quality has no monotonic trend as observed, and the exact relationship should be elucidated by studying the fluid dynamics of this printing process in a future study.

Overall, the printing quality is influenced by the fluid properties, and this influence is further illustrated in figure 8 as the sodium alginate concentration and laser fluence change. Generally, the tube wall thickness and tube outer diameter decrease with the sodium alginate concentration, while they first increase, then decrease and finally increase again with the laser fluence. The tube wall thickness and outer diameter are more sensitive to the change of sodium alginate concentration under lower laser fluences. Similarly, the tube wall thickness and outer diameter are more sensitive to the change of laser fluence when using lower concentration sodium alginate solutions. In other words, the sodium alginate concentration dominates if the laser fluence is low, and the laser fluence dominates if the sodium alginate concentration is low.

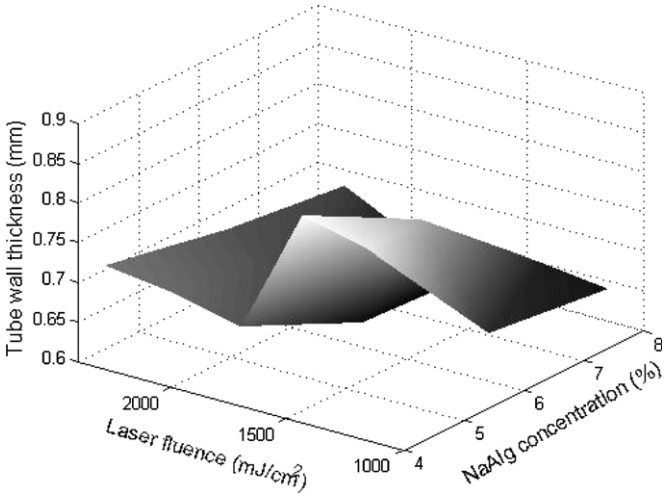

Figure 8. Tube wall thickness as functions of laser fluence and sodium alginate concentration.

3.4. Effect of laser spot size

Intuitively, the feature size should be reduced by using a smaller laser spot size. The effect of spot size on the printing quality has also been examined, and the results are shown in figure 7 when two different spot sizes (150 versus 50 μm in diameter) were tested. Under the same laser fluence, the incident energy decreased as the spot size was smaller. As expected, both the tube wall thickness and outer diameter reduced as the laser spot size decreased since fewer materials were transferred per pass. However, it can be seen that the thickness did not reduced to one third as the spot size reduced to one third (from 150 to 50 μm) and the thickness reduction was more pronounced at higher laser fluences. This observation is attributed to the following reason. The spreading effect after landing may be the dominating effect on the printing quality, overshadowing that of the jet/droplet size. On the other hand, this spreading effect is less significant when the jet/droplet is more viscous as with high concentration sodium alginate solutions.

Varying the laser spot size demonstrates the possibility of improving the printing quality; however, there are some concerns with this approach. First, the printing productivity may decrease since each deposited layer is thinner, and more layers are needed for a given construct. Second, a higher laser fluence might be needed for effective transfer since the energy per pulse is the product of laser fluence and laser spot size. Higher laser fluences may lead to more cell damage [14, 20] during the printing of cellular constructs. In addition, slim constructs may buckle or collapse, so sometimes it is expected to use a relatively larger spot size to have a thick structure.

4. Conclusions and future work

Laser-assisted printing such as LIFT has been well studied to pattern or fabricate 2D constructs, while there is no investigation on its 3D printing performance. This study has investigated the effects of sodium alginate concentration and operating conditions such as the laser fluence and laser spot

size on the printing quality during laser-assisted printing of alginate tubes with a nominal diameter of 3 mm. It is found that highly viscous materials can be printed into well-defined tubular constructs. As discussed, the printing quality is affected by the fluid properties and operating conditions. The tube wall thickness and tube outer diameter decrease with the sodium alginate concentration, while first increasing, then decreasing and finally increasing again with the laser fluence. The sodium alginate concentration dominates if the laser fluence is low, and the laser fluence dominates if the sodium alginate concentration is low.

For better biomedical applications of laser-assisted printing, future work may include: (1) the automation of printing process to achieve a higher efficiency, (2) time-resolved imaging study of the jet and droplet formation of viscoelastic fluids including alginate solutions, (3) use of sacrificial layer(s) for process improvement, and (4) the development of mathematical models accounting for the entire printing process including jet/droplet formation, landing, spreading and gelation. In addition, other organ printing-related topics might be of interest such as the maximum size of obtainable biological constructs, the behavior of the construct being built in the solution/container over a longer period of time and the change of properties of the solution with the volume of the construct being built.

Acknowledgments

The study was partially supported by the National Science Foundation (CMMI-CAREER 0747959 and EPS-0903795). The authors would like to acknowledge the experimental assistance by Hemanth Gudapati, Changxue Xu and Wenxuan Chai of Clemson University.

References

[1] Mironov V *et al* 2009 Organ printing: tissue spheroids as building blocks *Biomaterials* **30** 2164–74
[2] Wilson W C and Boland T 2003 Cell and organ printing 1: protein and cell printers *Anat. Rec.* A **272A** 491–6
[3] Riggs B C *et al* 2011 Matrix-assisted pulsed laser methods for biofabrication *MRS Bull.* **36** 1043–50
[4] Wüst S, Müller R and Hofmann S 2011 Controlled positioning of cells in biomaterials—approaches towards 3D tissue printing *J. Funct. Biomater.* **2** 119–54
[5] Boland T *et al* 2007 Drop-on-demand printing of cells and materials for designer tissue constructs *Mater. Sci. Eng.* C **27** 372–6
[6] Wohlers T 2001 Wohlers report 2001: rapid prototyping and tooling, state of the industry Annual Worldwide Progress *Report* (Wohlers Associates, Fort Collins, CO)
[7] Boland T, Xu T, Damon B and Cui X 2006 Application of inkjet printing to tissue engineering *Biotechnol. J.* **1** 910–7
[8] Nishiyama Y *et al* 2009 Development of a three-dimensional bioprinter: construction of cell supporting structures using hydrogel and state-of-the-Art inkjet technology *J. Biomech. Eng.* **131** 035001
[9] Xu C, Chai W, Huang Y and Markwald R R 2012 Scaffold-free inkjet printing of three-dimensional zigzag cellular tubes *Biotechnol. Bioeng.* **109** 3152–60
[10] Norman J J and Desai T A 2006 Methods for fabrication of nanoscale topography for tissue engineering scaffolds *Ann. Biomed. Eng.* **34** 89–101
[11] Herran L C and Huang Y 2012 Alginate microsphere fabrication using bipolar wave-based drop-on-demand jetting *J. Manuf. Process.* **14** 98–106
[12] Herran L C, Huang Y and Chai W 2012 Performance evaluation of bipolar and tripolar excitations during nozzle-jetting-based alginate microsphere fabrication *J. Micromech. Microeng.* **22** 085025
[13] Barron J A *et al* 2005 Printing of protein microarrays via a capillary-free fluid jetting mechanism *Proteomics* **5** 4138–44
[14] Lin Y, Huang Y, Wang G, Tzeng T J and Chrisey D B 2009 Effect of laser fluence on yeast cell viability in laser-assisted cell transfer *J. Appl. Phys.* **106** 043106
[15] Koch L *et al* 2010 Laser printing of skin cells and human stem cells *Tissue Eng. C* **16** 847–54
[16] Schiele N R *et al* 2010 Laser-based direct-write techniques for cell printing *Biofabrication* **2** 032001
[17] Lin Y and Huang Y 2011 Laser-assisted fabrication of highly viscous alginate microsphere *J. Appl. Phys.* **109** 083107
[18] Barron J A, Ringeisen B R, Kim H, Spargo B J and Chrisey D B 2004 Application of laser printing to mammalian cells *Thin Solid Films* **453–4** 383–7
[19] Ringeisen B R *et al* 2004 Laser printing of pluripotent embryonal carcinoma cells *Tissue Eng.* **10** 483–91
[20] Lin Y, Huang G, Huang Y, Tzeng T J and Chrisey D B 2010 Effect of laser fluence in laser-assisted direct writing of human colon cancer cell *Rapid Prototyping J.* **16** 202–8
[21] Lin Y, Huang Y and Chrisey D B 2009 Droplet formation in matrix-assisted pulsed-laser evaporation direct writing of glycerol-water solution *J. Appl. Phys.* **105** 093111
[22] Guillemot F, Souquet A, Catros S and Guillotin B 2010 Laser-assisted cell printing: principle, physical parameters versus cell fate and perspectives in tissue engineering *Nanomedicine* **5** 507–15
[23] Gruene M *et al* 2011 Laser printing of stem cells for biofabrication of scaffold-free autologous grafts *Tissue Eng. C* **17** 79–87
[24] Catros S *et al* 2011 Laser-assisted bioprinting for creating on-demand patterns of human osteoprogenitor cells and nano-hydroxyapatite *Biofabrication* **3** 025001
[25] Koch L *et al* 2012 Skin tissue generation by laser cell printing *Biotechnol. Bioeng.* **109** 1855–63
[26] Mironov V, Boland T, Trusk T, Forgacs G and Markwald R R 2003 Organ printing: computer-aided jet-based 3D tissue engineering *Trends Biotechnol.* **21** 157–61
[27] Khalil S, Nam F and Sun W 2005 Multi-nozzle deposition for construction of 3D biopolymer tissue scaffolds *Rapid Prototyping J.* **11** 9–17
[28] Phamduy T B *et al* 2012 Laser direct-write of single microbeads into spatially-ordered patterns *Biofabrication* **4** 025006
[29] Young D, Auyeung R C Y, Piqué A, Chrisey D B and Dlott D D 2002 Plume and jetting regimes in a laser based forward transfer process as observed by time-resolved optical microscopy *Appl. Surf. Sci.* **197–8** 181–7
[30] Duocastella M, Fernández-Pradas J M, Serra P and Morenza J L 2008 Jet formation in the laser forward transfer of liquids *Appl. Phys.* A **93** 453–6
[31] Serra P, Duocastella M, Fernández-Pradas J M and Morenza J L 2009 Liquids microprinting through laser-induced forward transfer *Appl. Surf. Sci.* **255** 5342–5
[32] Wang W, Li G and Huang Y 2009 Modeling of bubble expansion-induced cell mechanical profile in laser-assisted cell direct writing *Trans. ASME J. Manuf. Sci. Eng.* **131** 051013
[33] Lin Y, Foy K, Huang Y and Chrisey D B 2008 Bubble formation modeling in matrix-assisted pulsed-laser evaporation direct write *MSEC 2008: Proc. ASME Int.*

Manufacturing Science and Engineering Conf. (Evanston, Illinois, USA) MSEC_ICMP2008-72241 pp 1–8

[34] Unger C, Gruene M, Koch L, Koch J and Chichkov B N 2011 Time-resolved imaging of hydrogel printing via laser-induced forward transfer *Appl. Phys.* A **103** 271–7

[35] Duocastella M, Fernández-Pradas J M, Morenza J L and Serra P 2009 Time-resolved imaging of the laser forward transfer of liquids *J. Appl. Phys.* **106** 084907

[36] Duocastella M, Fernández-Pradas J M, Morenza J L and Serra P 2010 Sessile droplet formation in the laser-induced forward transfer of liquids: a time-resolved imaging study *Solid Thin Films* **518** 5321–5

[37] Herran L C, Wang W, Huang Y, Mironov V and Markwald R 2010 Parametric study of acoustic excitation-based glycerol–water microsphere fabrication in single nozzle jetting *Trans. ASME J. Manuf. Sci. Eng.* **132** 051001